

# The *C. elegans* LAR-like receptor tyrosine phosphatase PTP-3 and the VAB-1 Eph receptor tyrosine kinase have partly redundant functions in morphogenesis

Robert J. Harrington<sup>1</sup>, Michael J. Gutch<sup>2,\*</sup>, Michael O. Hengartner<sup>2</sup>, Nicholas K. Tonks<sup>2</sup> and Andrew D. Chisholm<sup>1,†</sup>

<sup>1</sup>Department of Molecular, Cell, and Developmental Biology, Sinsheimer Laboratories, University of California, Santa Cruz, CA 95064, USA

<sup>2</sup>Cold Spring Harbor Laboratory, 1 Bungtown Road, Cold Spring Harbor, NY 11724, USA

\*Present address: Electronic Publishing Services Inc., 880 Third Avenue, 14th Floor, New York, NY 10022, USA

†Author for correspondence (e-mail: chisholm@biology.ucsc.edu)

Accepted 16 January 2002

## SUMMARY

Receptor-like protein-tyrosine phosphatases (RPTPs) form a diverse family of cell surface molecules whose functions remain poorly understood. The LAR subfamily of RPTPs has been implicated in axon guidance and neural development. Here we report the molecular and genetic analysis of the *C. elegans* LAR subfamily member PTP-3. PTP-3 isoforms are expressed in many tissues in early embryogenesis, and later become localized to neuronal processes and to epithelial adherens junctions. Loss of function in *ptp-3* causes low-penetrance defects in gastrulation and epidermal development similar to those of

VAB-1 Eph receptor tyrosine kinase mutants. Loss of function in *ptp-3* synergistically enhances phenotypes of mutations in the *C. elegans* Eph receptor VAB-1 and a subset of its ephrin ligands, but does not show specific interactions with several other RTKs or morphogenetic mutants. The genetic interaction of *vab-1* and *ptp-3* suggests that LAR-like RPTPs and Eph receptors have related and partly redundant functions in *C. elegans* morphogenesis.

Key words: Eph receptor, Phosphatase, RPTP, LAR, Morphogenesis, *C. elegans*

## INTRODUCTION

Receptor-like protein-tyrosine phosphatases (RPTPs) form a diverse family of transmembrane enzymes that play roles in cell adhesion and cell signaling (Brady-Kalnay and Tonks, 1995; den Hertog et al., 1999). The LAR (Leukocyte Common Antigen Related) protein is the founding member of a subfamily of RPTPs known as type IIa RPTPs, defined by extracellular domains composed of immunoglobulin-like and fibronectin type III (FNIII) domains. The extracellular domain of LAR thus resembles those of cell adhesion proteins such as N-CAM, implying that it links cell adhesion and intracellular tyrosine phosphorylation.

Vertebrate genomes contain at least three LAR-like RPTP genes: LAR, PTP $\delta$ , and PTP $\sigma$ . All three generate multiple protein isoforms by tissue-specific alternative splicing, and are expressed in complex patterns in many ectodermal and endodermal epithelia and in neural tissues (Pulido et al., 1995; Stoker and Dutta, 1998). In non-neuronal cells LAR family members localize to focal adhesions (Serra-Pagès et al., 1995), adherens junctions (Aicher et al., 1997) and regions in contact with basal laminae. In neurons, LAR family members are found on cell bodies, processes and growth cones, suggesting a role in modulating cell adhesion during axon outgrowth

(Zhang et al., 1998; Zhang and Longo, 1995). The *Drosophila* LAR ortholog Lar (previously known as Dlar), is mostly expressed in the nervous system (Krueger et al., 1996), although expression in oogenesis has also been observed (Fitzpatrick et al., 1995).

The most detailed analysis of RPTP function in vivo has been in *Drosophila*. In mutants lacking Lar some motor axons bypass their correct target area, reflecting a failure in defasciculation at the point where the axons choose to extend into the muscle (Krueger et al., 1996). Lar is also required for normal target recognition by axons from retinal photoreceptors; in *Lar* mutants, these axons retract from their normal target layer, suggesting a role for Lar in recognition or adhesion to target layer cells (Clandinin et al., 2001; Maurel-Zaffran et al., 2001). Different defasciculation or outgrowth defects are seen in fly mutants lacking other RPTPs (Desai et al., 1996; Garrity et al., 1999; Sun et al., 2000a). The axonal phenotypes observed in *Lar* mutants are incompletely penetrant, likely because other RPTPs can substitute for loss of Lar function (Desai et al., 1997). Thus, in *Drosophila*, Lar functions to modulate cell adhesion during axon growth; several likely components of the Lar pathway have recently been identified based on their interactions with Lar in growth cone guidance (Bateman et al., 2000; Wills et al., 1999). Lar

has also recently been found to play roles in early embryonic morphogenesis in *Drosophila*, where it functions in polarization of somatic follicle cells (Bateman et al., 2001; Frydman and Spradling, 2001).

Mice lacking Lar have defects in mammary gland development (Schaapveld et al., 1997) and in glucose homeostasis (Ren et al., 1998), and have mild defects in the CNS (Yeo et al., 1997). Mice lacking PTP $\delta$  display mild neural and epithelial defects, including a slight decrease in brain size and reduction in the size of the posterior pituitary (Elchebly et al., 1999; Wallace et al., 1999); the cellular basis of these defects is unknown. PTP $\delta$  mutant mice display defects in spatial learning, yet show no neuroanatomical defects (Uetani et al., 2000).

The *C. elegans* genome contains 26 receptor protein-tyrosine phosphatases, including orthologs of most major vertebrate RPTP classes (Plowman et al., 1999; Wälchli et al., 2000). We report here the characterization of PTP-3, the *C. elegans* ortholog of the LAR subfamily. We identify a loss-of-function mutation in *ptp-3*, and show that this mutation causes defects in epidermal and early neural morphogenesis, although axon morphology in selected neurons appears normal. Epidermal and neural morphogenesis also require signaling via the *C. elegans* Eph receptor VAB-1 and its ephrin ligands (Chin-Sang et al., 1999; George et al., 1998; Wang et al., 1999). We find that *ptp-3* and Eph signaling mutations show specific synergistic effects on morphogenesis. Our results suggest that in *C. elegans* PTP-3/LAR and VAB-1/Eph RTK pathways play partly redundant roles in morphogenesis, and raise the possibility that LAR type RPTPs and Eph RTKs play redundant roles in other animals.

## MATERIALS AND METHODS

### *C. elegans* genetics

*C. elegans* worms were cultured as described by Brenner (Brenner, 1974), at 20°C unless stated otherwise. Mutations used were: LGII: *vab-1(e2, e116, e118, e699, dx31, e2027, tn2)*, *clr-1(e1745ts)*, *tra-2(q122dm)*, *unc-4(e120)*, *sqt-1(sc1sd)*; LGIII: *ina-1(gm119)*, *daf-2(e1370)*; LGIV: *efn-1(vab-2(ju1))*, *efn-2(ev658)*. LGX: *egl-15(n484)*, *efn-3(ev696)*. Rearrangements used were: LGII: *mnDf57*, *mnDf83*, *mnDf89*, *mnDf90*, *mnC1*, *mIn1* (previously known as *mC6*). Mutations not referenced in the text have been previously described (Riddle et al., 1997).

We constructed *vab-1 ptp-3* double mutants by recombination. Typically, progeny of *vab-1 unc-4/ptp-3* heterozygotes were screened for Vab non-Unc recombinants. Recombinants were homozygosed, if possible, and presence of the *op147* Tc1 insertion confirmed by PCR. Inviolate double mutants were maintained heterozygous to the balancer chromosomes *mnC1* or *mIn1* (Edgley and Riddle, 2001). *mIn1* balances the *vab-1* to *ptp-3* interval; a version of *mIn1* containing the GFP transgene *mIs14* were also used in later genetic constructions.

To construct double mutants with unlinked mutations of similar phenotypes, and to obtain balanced strains in the event of a synthetic-lethal interaction, we used the *mIn1 mIs14* balancer, or other dominant markers on LGII to follow the *ptp-3(+)* chromosome. For example, to make *ptp-3; ina-1* double mutants we crossed *tra-2(q122gf)* males with *ptp-3* hermaphrodites and obtained *ptp-3/tra-2* male cross progeny, which we mated with *sqt-1; ina-1* animals. The non-male F<sub>1</sub> progeny of this cross are either Roller females, of genotype *tra-2(q122)/sqt-1; ina-1/+*, or are Roller hermaphrodites, of genotype

*ptp-3/sqt-1; ina-1/+*. Such Rol F<sub>1</sub> hermaphrodites were selfed and Rol Egl F<sub>2</sub> animals selected, putatively homozygous for *ina-1* and heterozygous for *ptp-3* (balanced over *sqt-1*). Non-Dpy Non-Rol F<sub>3</sub> progeny were picked, putatively *ptp-3; ina-1*, and their progeny checked by PCR for homozygosity of the *op147* insertion.

Quantitation of lethality and statistical analysis of differences in lethality between strains were performed as described previously (Chin-Sang et al., 1999). For viable strains shown in Fig. 7, at least three complete broods (>500 animals) were quantitated with the aid of a dissecting microscope. For balanced synthetic-lethal strains, estimations of lethality were based on counts of eggs spot-checked using Nomarski microscopy; heterozygous animals and balancer homozygotes were viable and excluded from counts based on expression of the *mIs14* transgene. The *vab-1* alleles *dx31*, *e2027*, *ju8*, *tn2*, *e856*, *e118* and *e116* caused 100% lethality in combination with *ptp-3(op147)*, as determined by counts of strains of genotype *vab-1 ptp-3/mIn1 mIs14*.

### *ptp-3*/deficiency heterozygote analysis

The following chromosomal deficiencies failed to complement *op147*, based on the presence of the Ptp-3 morphology defects in cross-progeny resulting from crosses of *op147* or *op147/+* males with deficiency heterozygotes: *mnDf83*, *mnDf89*, *mnDf90*. The deficiency *mnDf57* complemented *op147*. To estimate the penetrance of lethal and morphological defects in *op147/Df* heterozygotes, we first generated strains in which the deficiencies were balanced in *trans* to *mIn1 mIs14*. Animals of genotype *Df/mIn1 mIs14* were feminized by feeding them bacteria expressing RNA for the *fem-1* gene, resulting in dsRNA-mediated interference (RNAi) of the endogenous *fem-1* gene (Timmons and Fire, 1998). Bacterial strain HT115, harboring the *fem-1* RNAi plasmid, was grown on NGM agar plates containing 1–10 mM IPTG and 25 µg/ml carbenicillin. One to two days later, L4 parental animals of genotype *Df/mIn1 mIs14* were placed on the plate. Feminized progeny were crossed with *op147* males; all non-GFP-expressing progeny from such a cross are of genotype *op147/Df*. The penetrance of lethal phenotypes in such animals was quantitated at 20°C as described above. Animals of genotype *op147/mnDf90* displayed 6.9% embryonic lethality and 3.3% larval morphology defects (*n*=360).

### RNA interference of *ptp-3*

A 1.3 kb *AccI-SacI* fragment from the *ptp-3* cDNA, corresponding to the C terminus of the intracellular domain, was subcloned into the L4440 RNAi vector. This construct was linearized to allow in vitro synthesis of the plus and minus strands in separate reactions (Promega Riboprobe Combination System-T7/T3). The reactions were combined and the resulting dsRNA (approx. 0.75–1 µg/µl) was injected into the gonad or gut of N2 hermaphrodites. The broods of 18 injected animals were scored for embryonic lethal and larval morphological defects; embryonic lethality in such broods averaged 4.6% (range 0 to 20.6%); larval abnormalities averaged 1.1% (range 0 to 9.1%).

### Four-dimensional microscopy

Timelapse microscopy in multiple focal planes (four-dimensional, 4-D) was performed as described previously (Chin-Sang et al., 1999). Movies were recorded at room temperature (approx. 22–23°C). We recorded movies from 37 *op147* embryos and 30 *vab-1(e2) op147* embryos derived from homozygous strains grown at 20°C. From balanced strains of genotype *vab-1 ptp-3(op147)/mIn1* we recorded movies from eleven *vab-1(dx31) ptp-3(op147)* embryos and six *vab-1(e2027) ptp-3(op147)* embryos.

### Cloning and molecular analysis of *ptp-3*

To analyze transcripts from *ptp-3* we made poly(A)<sup>+</sup> mRNA from approximately 80 µg of total RNA isolated from mixed stage N2 animals. This RNA was electrophoresed in a 1.5% formaldehyde

agarose gel and blotted using standard procedures (Sambrook et al., 1989). The blot was hybridized with a  $^{32}\text{P}$ -labeled *ptp-3B* cDNA.

We isolated a cDNA encoding the PTP-3B isoform by screening a  $\lambda$ ZAP library (kindly provided by R. Barstead) with a PTP-3 PCR clone. Primers PTP1-5 (5'CCCGAAGCGCCCGAGATCG) and PTP1-6 (5'CGGTTCCGTCGACTGTCTTCGCC) were used in PCRs using cosmid F38A3 as template, yielding the expected 183 bp *ptp-3* PCR fragment. This fragment was labeled with [ $\alpha$ - $^{32}\text{P}$ ]dATP and [ $\alpha$ - $^{32}\text{P}$ ]dCTP, and used to screen approx. 100,000 plaques using standard procedures (Sambrook et al., 1989). Three positives were identified and their inserts isolated. The longest *ptp-3* cDNA contained a 5' UTR of 80 bp, a coding region of 4461 bp, and a 3' UTR of 467 bp.

We used RT-PCR to generate cDNA clones of the PTP-3A transcript. For cDNA synthesis, we used primer oBH-18 (exon 18) (5'TCGTACTGAACATCAATCGGTTCCAC 3') as the anchor primer. We carried out the RT reaction at 37°C for 1 hour using 6  $\mu\text{g}$  of total N2 RNA, the anchor primer, and Superscript II Reverse Transcriptase (Gibco BRL). To amplify the fragments we used Vent DNA Polymerase (New England Biolabs) and the oBH-18 cDNA template in PCR reactions with the following combinations of primers.

To make the 847 bp fragment corresponding to exons 13-18, excluding 14, we used the oBH-18 primer in combination with primer oBH-19 (5'AGTACGACGAGGATATGGACG3'). This fragment was cloned into the *EcoRV* site of pBluescript. For the 1328 bp fragment that corresponds to exons 3-13, we used the following primers: oBH-33 (exon 6) (5'ACTTGACGATCCTTCTACTGC3') and oBH-31 (exon 13) (5'ATCCATCCATTGTCGACGCTGC3'). For the 1146 bp fragment we used the following primers: oBH-29 (Exon 1) (5'ATGAATCGGATAGCGCGTCACTTACG3') and oBH-32 (exon 6) (5'TGTTTCCGAGAGCACTGACAGC3'). Both of these products were cloned (using an *NcoI* site in exon 6) into pSL1190, using the *EcoRV* site as a blunt end site for the end opposite the *NcoI* site. RT-PCR clones were sequenced to confirm that no mutations were introduced in the PCR. We found no evidence for alternative splicing of the *ptp-3* locus, although our analysis was not exhaustive.

To test whether the genomic cosmid clone F38A3 could rescue *ptp-3* mutant phenotypes, we generated transgenic arrays by transforming wild-type animals with F38A3 (2 ng/ $\mu\text{l}$ ) and the plasmid pRF4 (30 ng/ $\mu\text{l}$ ), which confers a Roller phenotype. We obtained several such extrachromosomal arrays in wild-type background, then introduced these arrays into a *vab-1(e2) ptp-3(op147)* mutant background by crossing. We homozygosed for the *vab-1* and *ptp-3* mutations and confirmed homozygosity by complementation tests for *vab-1* and by PCR to detect *op147::Tc1*. The *e2 op147* double mutant displays approx. 81% embryonic lethality. If the transgenic arrays completely rescued *ptp-3* mutant phenotypes the embryonic lethality in transgenic animals should be at most suppressed to the level found in a *vab-1(e2) ptp-3(+)* strain, which is approx. 10.2% (George et al., 1998). Of four such arrays, three (*juEx183*, *juEx184*, *juEx186*) showed significant rescue of the *vab-1 ptp-3* synthetic lethality (Fig. 5); these arrays did not rescue the phenotypes of *vab-1(e2)* single mutants (not shown). Two integrated versions of *juEx183*, *juIs138* and *juIs139*, were generated by UV/trimethylpsoralen mutagenesis.

### Identification of *op147::Tc1*

We identified a Tc1 insertion in the PTP-3 coding region by screening the mutator strain MT3126 with primers specific to Tc1 and to the phosphatase domain of *ptp-3*, essentially as described previously (Gutch et al., 1998). Two sets of *ptp-3* primer pairs (sequences available on request) were used with Tc1-specific primers to screen 2880 cultures. A single *Tc1* insertion mutation was identified and worms homozygous for the insertion allele isolated. The *op147::Tc1* insertion allele was outcrossed 10 times to N2 prior to phenotypic and genetic analyses. By sequencing the insertion site we determined that Tc1 had inserted between nucleotides 9486 and

9487 of the F38A3 clone, the flanking sequence being 5' GAAGCT[*op147::Tc1*]ACATTG 3'.

### Construction of PTP-3 GFP reporter genes and transgenic strains

#### Construction of PTP-3B::GFP

To create the *ptp-3B::GFP* minigene, a unique *PstI* site in the *ptp-3B* cDNA immediately 3' to the coding region for the second phosphatase domain was used to insert GFP coding sequence (GFP variant F64L S65T, derived from vectors generously provided by A. Fire) in frame with the PTP-3B protein (clone pBH8). A 14651 bp *NcoI-NorI* fragment from cosmid F38A3, corresponding to the *ptp-3B* promoter and exons 14-20 (Fig. 1A) was cloned into pSL1190 (pBH1). From pBH8 a 5 kb *NorI* fragment was cloned into the *NorI* site of pBH1. The resulting clone, pCZ406, contains genomic sequence for the promoter and the first approx. 6.5 exons of PTP-3B; the second half of exon 19 and subsequent exons are present as cDNA, tagged with GFP.

We made two series of transgenic arrays containing the PTP-3B::GFP minigene. The first series was formed by injection of pCZ406 at high concentrations (50 ng/ $\mu\text{l}$ ), together with the marker plasmid pRF4 (30 ng/ $\mu\text{l}$ ). Four such 'high concentration' arrays, *juEx188* through *juEx191*, gave robust GFP expression and caused low-penetrance morphogenetic defects in wild-type genetic backgrounds and sickness and inviability in *vab-1 ptp-3* mutant backgrounds. A second series of transgenes was therefore generated by injection of the PTP-3B::GFP minigene at low concentrations (5 ng/ $\mu\text{l}$ ), together with pRF4 (30 ng/ $\mu\text{l}$ ). Such 'low concentration' arrays gave weak GFP fluorescence; GFP expression in a pattern similar to that of the high-concentration arrays could be detected by immunostaining with anti-GFP antibodies (not shown). The low concentration arrays (*juEx222-juEx224*) did not cause lethality in wild-type or *vab-1 ptp-3* mutant backgrounds and were used to assay rescuing activity of the transgenes.

#### Construction of Ptp-3A::GFP

A 5090 bp DNA fragment corresponding to the putative *ptp-3A* promoter and ATG was amplified from N2 genomic DNA using Long PCR (Boehringer Mannheim) and cloned into the *PstI* and *BamHI* sites of pPD122.34 using sites engineered into the primers; sequences of primers used are available on request. This construct was injected into N2 hermaphrodites at 50 ng/ $\mu\text{l}$  with the pRF4 marker plasmid (30 ng/ $\mu\text{l}$ ).

### Tissue-specific expression of PTP-3B

To make constructs expressing PTP-3B under the control of the *unc-119* or *jam-1* promoters we amplified appropriate promoter regions using PCR and cloned them into constructs containing the PTP-3B cDNA. Details of primer sequences and plasmid constructions are available on request. Transgenic arrays were established by coinjection of the appropriate promoter construct (5 ng/ $\mu\text{l}$ ) and a SUR-5-GFP marker plasmid (30 ng/ $\mu\text{l}$ ) into N2 wild-type animals. Arrays were introduced into a *vab-1(e2) ptp-3(op147)* background by crossing and penetrance of morphogenetic phenotypes quantitated as described above.

### Anti-PTP-3 antibodies and immunostaining

A 2.1 kb PCR product corresponding to the entire PTP-3 intracellular domain (residues 1509-2190) was amplified from the *ptp-3* cDNA using primers introducing *NorI* and *SalI* sites. The PCR product was digested with *NorI* and *SalI* and cloned into pGEX4T-3 (Amersham), yielding a clone that fuses the PTP-3 intracellular domain with GST. The fusion protein antigen was purified from 6 liters of induced *E. coli* DH5 $\alpha$  using a protocol developed by Doug Kellogg (Carroll et al., 1998), and used to immunize rabbits (Animal Pharm). Bleeds were tested for immunoreactivity against purified GST-PTP-3. 10 ml of serum from the most immunoreactive bleed was purified by

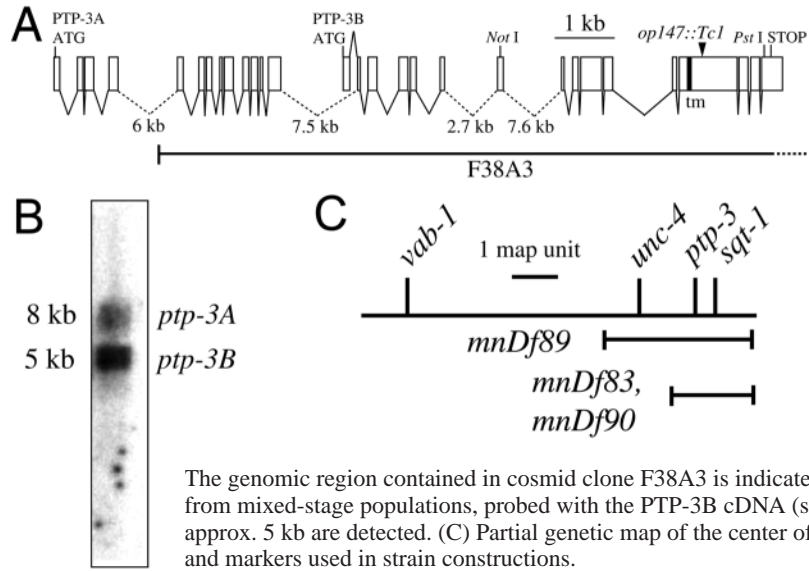


**Fig. 1.** Structure of the *ptp-3* locus. (A) Genomic structure of the *ptp-3* locus and location of *op147::Tc1*. The long transcript, encoding PTP-3A, is generated from 29 coding exons that span 36.2 kb of genomic DNA; this transcription unit is denoted C09D8.1 in the *C. elegans* genome database (also previously known as *clar*, *ypp-1*, and *ptp-1*). Four large introns are not shown to scale (dotted lines). Exons 1-13 are specific to the long transcript. Exon 14 contains the ATG for the short transcript and is transcribed from an internal promoter. Exon 13 (PTP-3A) or exon 14 (PTP-3B) both splice to exon 15. Exons 15-30 are common to both transcripts. The transmembrane domain (tm) and the D1 phosphatase domain are encoded by exon 26. The Tc1 insertion of *op147* is in exon 26, disrupting the D1 phosphatase domain. The *PstI* site used to insert GFP is indicated.

(B) Northern blot of total *C. elegans* mRNA extracted from mixed-stage populations, probed with the PTP-3B cDNA (see Materials and Methods). Messages of approx. 8 kb and approx. 5 kb are detected. (C) Partial genetic map of the center of linkage group II, showing map location of *ptp-3*, *vab-1*, and markers used in strain constructions.

adsorption to purified GST-PTP-3 blotted onto nitrocellulose, followed by washing and dialysis into 1× PBS, 50% glycerol, following standard procedures (Harlow and Lane, 1999). The resulting affinity purified serum was used at 1 in 100 dilution for immunostaining. Staining was carried out using a version of the Finney-Ruvkun fixation protocol (Finney and Ruvkun, 1990) optimized for embryos. Embryos were immunostained with MH27 and anti-GFP antibodies as described previously (Chin-Sang et al., 1999). Images were acquired on a Leica TCS-NT confocal microscope or a Zeiss Axioplan 2.

## RESULTS

### The *ptp-3* locus encodes two isoforms of a *C. elegans* LAR-like RPTP

We identified the *ptp-3* gene in a PCR-based screen for *C. elegans* genes encoding protein tyrosine phosphatases (Gutch et al., 1998). The genomic sequence of the *ptp-3* locus was determined by the *C. elegans* genome consortium, and is contained in cosmid clones C09D8 and F38A3 (Fig. 1A). Using northern blots of *C. elegans* mRNA we found that the *ptp-3* locus generates two major transcripts, of approximately 8 kb and 5 kb (Fig. 1B). We determined the sequences of cDNAs corresponding to these two transcripts as described in Materials and Methods. Comparison of *ptp-3* cDNA and genomic sequences revealed that the two transcripts have common 3' sequences and differ in their 5' ends. This difference arises from the use of alternative promoters and sets of 5' exons, as shown in Fig. 1A. The long transcript encodes a 2190 amino acid polypeptide designated PTP-3A, and the shorter *ptp-3* transcript encodes a 1487 residue polypeptide designated PTP-3B. Exons 15 through 29 are common to both transcripts and encode the C-terminal 1452 residues common to both isoforms.

PTP-3A, like other LAR-like (type IIa) RPTPs, has an extracellular domain consisting of three N-terminal immunoglobulin-like (Ig) domains and eight fibronectin type III (FNIII) repeats, and an intracellular domain containing two protein-tyrosine phosphatase (PTP) domains. Within all these domains, the closest relative to PTP-3A is DLAR; vertebrate

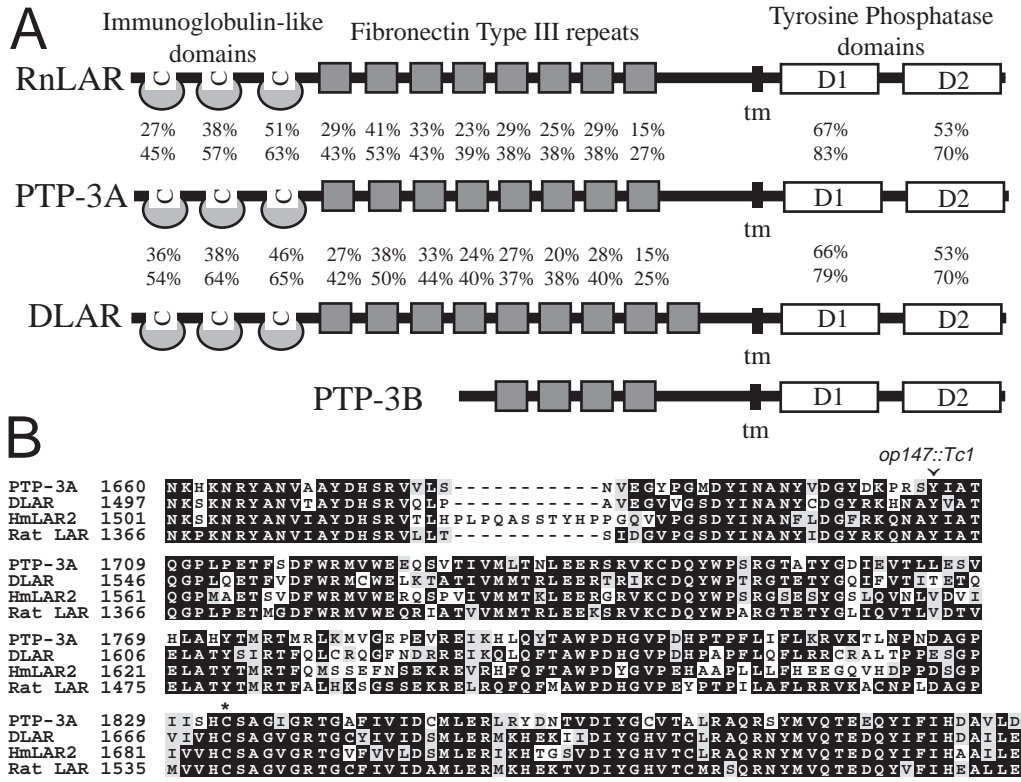
LAR-like proteins are slightly less similar (Fig. 2A,B). The smaller isoform, PTP-3B, lacks the N-terminal Ig domains and the four N-terminal FNIII repeats (Fig. 2A). Other LAR family genes generate multiple isoforms by alternative splicing, but none appears to use internal promoters to generate isoforms of the same domain structure as PTP-3B.

### PTP-3 isoforms are widely expressed in early development and are later predominantly expressed in the nervous system

To learn where PTP-3 was expressed during development we generated animals expressing PTP-3::GFP transgenes (see Materials and Methods). PTP-3B::GFP transgenes partly rescued the defects of *ptp-3* mutants (see below; Fig. 5A), suggesting that it reproduces part of the endogenous PTP-3B expression pattern. To identify the cells in which PTP-3A was expressed we used transcriptional fusion constructs that expressed GFP under the control of *ptp-3A* upstream sequences.

PTP-3B::GFP transgenes showed widespread expression in embryos. The earliest stage at which we detected GFP fluorescence in these embryos was during late gastrulation (approximately 250-300 minutes after first cleavage at 20°C). PTP-3B::GFP expression was observed uniformly on the surface of most, possibly all, cells in the embryo during gastrulation cleft closure and epidermal enclosure (Fig. 3A,D). In later embryos, larvae and adults PTP-3B::GFP expression became highest in the nervous system, including the nerve ring, dorsal cord, and ventral cord (Fig. 3G-I). PTP-3B::GFP was expressed in many but not all neurons, within which it was localized to neurites. In later embryos and larvae PTP-3B-GFP became localized within epidermal cells, apparently to adherens junctions (data not shown). The *Pptp-3A*::GFP construct expressed GFP from the comma stage (380 minutes) onwards in many neurons that also expressed PTP-3B::GFP (data not shown). Thus, PTP-3 isoforms are expressed in many tissues during early development, and later become restricted to the nervous system and epithelial tissues. To determine the expression of endogenous PTP-3 proteins we raised antibodies against the intracellular domain of PTP-3; these antisera are

**Fig. 2.** PTP-3 is the *C. elegans* ortholog of the LAR subfamily. (A) Percentage identity and similarity of PTP-3A Immunoglobulin-like (Ig-like) domains, Fibronectin Type III (FNIII) repeats, and phosphatase domains to those of its closest relative (DLAR), and a representative vertebrate LAR family member (rat LAR). The PTP-3B isoform is also shown for comparison; cartoons are not to scale. DLAR contains a ninth FNIII repeat; the FNIII domains of PTP-3 align with the first eight repeats of DLAR. PTP-3A is the largest member of the LAR family; the extra size is mostly due to a larger 'spacer' region between the last FNIII repeat and the predicted transmembrane domain. Percentages are calculated from alignments using ClustalW. (B) Alignment of the N-terminal (D1) phosphatase domain of PTP-3 with those of other LAR family members (DLAR, HmLAR2, and rat LAR), using ClustalW. Within the phosphatase domains, DLAR is the most similar protein to PTP-3; within the vertebrate LAR family, PTP $\delta$  proteins are slightly more similar to PTP-3 than are LAR or PTP $\gamma$ . The *op147* insertion disrupts codon Y1705 in the first phosphatase domain, between the conserved residues YINAN and FWRM. The predicted catalytic cysteine residue C1833 is marked (asterisk). Accession numbers are M27700 (DLAR), AF017083 (HmLAR2), and S46216 (rat LAR). The sequences of PTP-3 cDNAs have been deposited in GenBank, with accession numbers AF316539 (PTP-3A) and AF316540 (PTP-3B).



expected to recognize both PTP-3 isoforms. The staining of anti-PTP-3 antisera in wild-type animals (Fig. 3G) was weaker, but otherwise identical in pattern to the expression pattern of the PTP-3B::GFP transgenes.

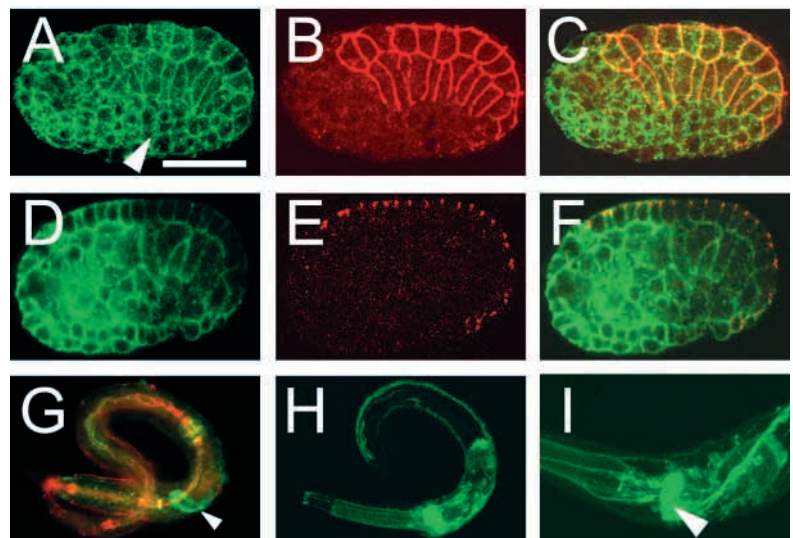
**Loss of *ptp-3* function results in defects in epidermal morphogenesis**

We generated a Tc1 transposon insertion mutation, *op147*, that

disrupts the first phosphatase domain of PTP-3. This mutation is therefore predicted to disrupt catalytic activity of both PTP-3 isoforms (see Materials and Methods). We show below that by genetic criteria the *op147* mutation behaves as a strong loss-of-function mutation in *ptp-3*.

Most *ptp-3(op147)* mutant animals appeared wild-type in morphology and behavior. The most obvious phenotype of *ptp-3(op147)* mutants was a variable and incompletely penetrant

**Fig. 3.** Embryonic and neuronal expression of PTP-3. (A-F) Expression of PTP-3B-GFP in enclosure stage embryos. Animals are of genotype *juEx189*; GFP is visualized by anti-GFP immunostaining (green), animals are also immunostained with MH27 to visualize adherens junctions (red). (A-C) A lateral confocal projection of an embryo prior to epidermal enclosure. The dorsal sheet of epidermal cells is visualised by MH27 staining; PTP-3B::GFP expression is widespread in surface cells; expression in ventral neuroblasts is marked in A (arrowhead). (D-F) A post-gastrulation embryo; medial confocal section showing widespread expression of PTP-3B::GFP at cell surfaces in epidermal, neuronal, pharyngeal, muscle, and endodermal tissue layers. (G) Wild-type L1 larva stained with anti-PTP-3 antibodies and MH27. Nerve ring staining is marked by the arrowhead. (H,I) PTP-3B-GFP expression in L1 (H) and adult (I) (*juEx189*), stained with anti-GFP antibodies; note intense nerve ring expression (arrowhead in I) and staining in neuronal processes. Scale bar, 10  $\mu$ m (A-F); 30  $\mu$ m (G, H); 100  $\mu$ m (I).



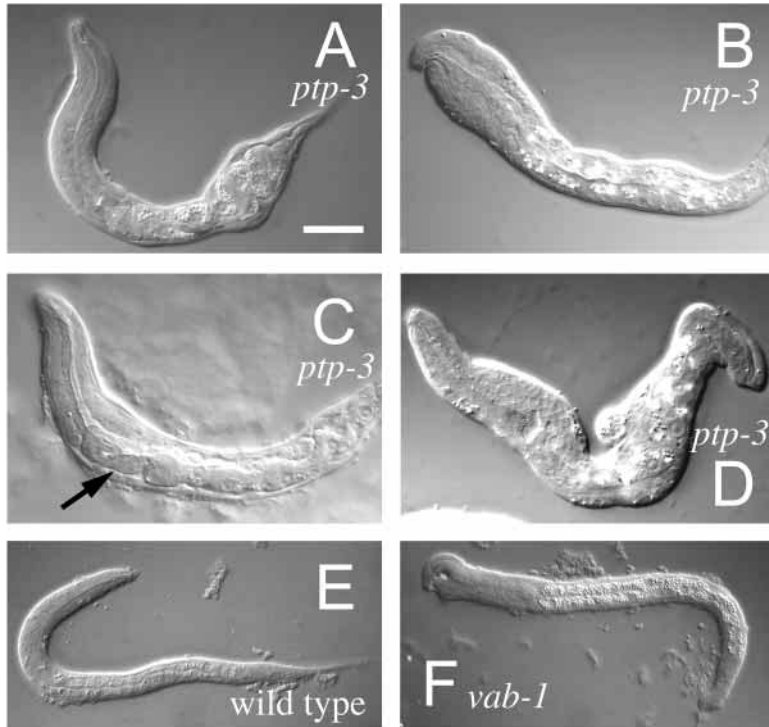


**Fig. 4.** Morphological phenotypes of *ptp-3* mutants. (A–D) Representative *ptp-3(op147)* mutant L1 stage larvae (grown at 25°C) showing defects in morphogenesis. The most common defect is a bulging or pinching of the posterior body (A); however, pinched or notched heads are also occasionally seen (B). Some inviable *ptp-3(op147)* larvae are starved, apparently a result of defects in pharyngeal morphogenesis (arrow in C). Some *ptp-3(op147)* larvae are deformed along the entire body (D). A wild-type L1 larva (E) and *vab-1(null)* mutant larva (F) showing the head morphology defect are shown for comparison. Scale bar, 13  $\mu\text{m}$  (A–D), 20  $\mu\text{m}$  (E,F).

defect in epidermal morphogenesis (Table 1; Fig. 4). At 20°C, 85% of *ptp-3* animals appeared morphologically wild type. The remaining 15% displayed variable defects in epidermal morphology; about one third of these animals arrested in embryogenesis (see below); one third arrested during larval development, and the remainder developed to adulthood. A common morphological defect in *ptp-3* larvae and adults was a swelling or blunting of the posterior epidermis (Fig. 4A). This ‘blunt posterior’ phenotype is similar to that observed in some animals mutant for the VAB-1 Eph receptor tyrosine kinase or the VAB-2/EFN-1 ephrin ligand (Fig. 4F). However, the distinctive anterior morphology defects (‘Notched head’) of *vab-1* or *vab-2* mutants were not seen in *ptp-3* mutants, which only occasionally displayed a swollen or pinched head region (Fig. 4B). The *op147* mutation is slightly temperature sensitive (Table 1).

We asked whether *op147* behaved genetically as a loss-of-function mutation by examining the phenotypes of animals heterozygous for *op147* in *trans* to chromosomal deficiencies spanning *ptp-3* (Fig. 1C). Such *op147/Df* animals displayed a similar range and penetrance of defects to those of *op147* homozygotes (see Materials and Methods). dsRNA-mediated interference of *ptp-3* caused morphogenetic defects similar to those of *ptp-3(op147)* mutants (see Materials and Methods).

**Table 1. Penetrance of *ptp-3(op147)* visible and lethal phenotypes**

Genotype, temperature (n)	Embryonic lethality	Larval lethality	Deformed adult	Wild-type
<i>ptp-3(op147)</i> 15°C (746)	4.1%	5.8%	2.3%	87.8%
<i>ptp-3(op147)</i> 20°C (945)	5.3%	5.0%	3.7%	85.8%
<i>ptp-3(op147)</i> 22.5°C (669)	5.1%	1.3%	3.3%	90.2%
<i>ptp-3(op147)</i> 25°C (462)	11.6%	8.2%	3.8%	76.1%

Taken together, these data suggest that *ptp-3(op147)* causes a strong loss of *ptp-3* function. However, the nature of the *op147* lesion suggests that it may not be a complete molecular null mutation in PTP-3, as Tc1 insertions in genes can be removed by splicing (Rushforth and Anderson, 1996) or somatic excision (Eide and Anderson, 1988). Consistent with this possibility, extremely weak anti-PTP-3 staining was observed in approx. 70% of *ptp-3(op147)* mutant animals; in the remaining 30%, anti-PTP-3 staining was completely absent. Finally, if PTP-3 has phosphatase-independent functions then these may be unaffected by *op147*.

To confirm that the mutant defects in *op147* strains were due to the *op147* mutation, we asked whether transgenic arrays containing *ptp-3(+)* genomic DNA could rescue *op147* mutant phenotypes. Transgenes containing cosmid F38A3 rescued *ptp-3* mutant phenotypes (Fig. 5A); because the *ptp-3(op147)* phenotype is weak, we assayed rescue of *vab-1 ptp-3* synthetic lethal phenotypes (see Materials and Methods). The F38A3 clone does not contain *ptp-3* exons 1–4 (see Fig. 1A) and thus cannot encode full-length PTP-3A. Thus, overexpression of PTP-3B can partly rescue the defects of *ptp-3(op147)* mutants. PTP-3B::GFP transgenes also displayed partial rescuing activity, consistent with these genomic rescue experiments (Fig. 5).

#### ***ptp-3* mutants are defective in embryonic neuroblast and epidermal movements, but display normal axon guidance in selected neurons**

The epidermal morphogenetic defects of *ptp-3* mutants arise during embryogenesis, and are reminiscent of those seen in *vab-1* and *efn-1* mutants. *vab-1* (Eph receptor) and *efn-1* (ephrin, previously *vab-2*) mutant embryos display defects in two phases of embryonic cell movements: closure of the ventral gastrulation cleft by short-range neuroblast movements, and enclosure of the embryo by epidermal cell shape changes (Chin-Sang et al., 1999; George et al., 1998). We therefore asked whether *ptp-3* mutant embryos were also defective in these embryonic morphogenetic processes.

Using four-dimensional (4-D) microscopy we found that *ptp-3* mutant embryos were defective in both closure of the gastrulation cleft and in epidermal enclosure (Fig. 6, second and third rows). Of 37 *ptp-3* mutant embryos recorded we observed defects in gastrulation cleft closure in seven; six of these seven subsequently failed to enclose the epidermis and arrested at the early enclosure stage of morphogenesis. The remaining 30 displayed normal gastrulation cleft closure and

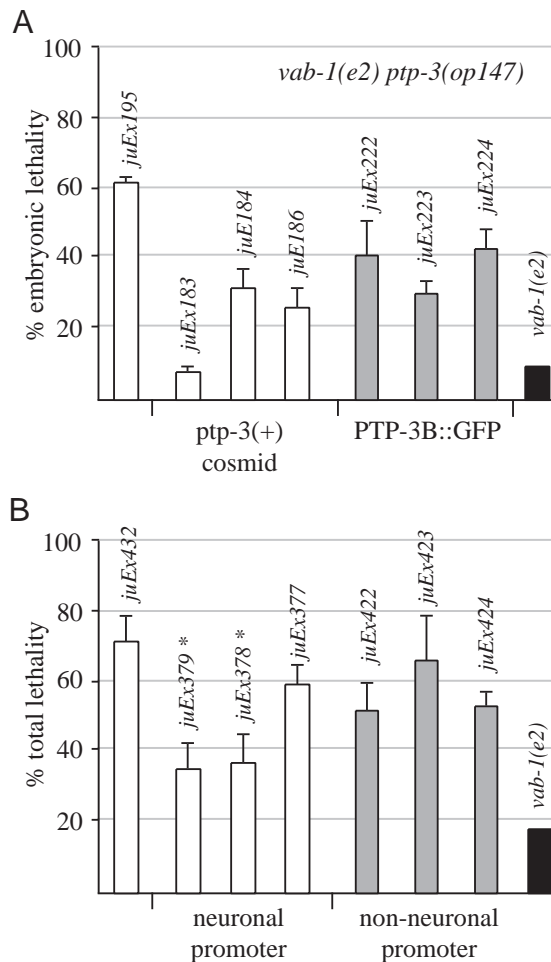


**Fig. 5.** Transgenic rescue of *vab-1 ptp-3* synthetic lethality by PTP-3B. Embryonic lethality was quantitated in transgenic strains as described in Materials and Methods. All strains are homozygous for *vab-1(e2)* and *ptp-3(op147)*. (A) *ptp-3(+)* transgenes (4 lines) contain the cosmid F38A3; PTP-3B::GFP transgenes (3 lines) contain the PTP-3B::GFP transgene injected at low concentration (see Materials and Methods). The *vab-1 ptp-3* synthetic lethality is suppressed in lines containing these transgenes, relative to control extrachromosomal arrays containing the pRF4 marker plasmid (*juEx195*). Data for *vab-1(e2)* (George et al., 1998) are shown for comparison. (B) Suppression of *vab-1 ptp-3* synthetic lethality by neuronally expressed PTP-3B (*juEx377-379*) but not by epidermally expressed PTP-3B (*juEx422-424*). Only arrays *juEx378* and *juEx379* caused significant reduction in lethality (Student's *t*-test,  $P < 0.01$ ).

epidermal morphogenesis. The defects in *ptp-3* mutants could be classified using the same criteria as used to classify *vab-1* or *efn-1* embryonic phenotypes (see Fig. 6 legend). Thus, *ptp-3* mutant embryos display low-penetrance defects in gastrulation and epidermal enclosure, similar to those observed in *vab-1* or *efn-1* mutants.

Genetic analysis in *Drosophila* has implicated RPTPs in axon guidance and fasciculation. We examined the process morphology of selected neurons (mechanosensory neurons and GABAergic motor neurons) in *ptp-3* mutants using GFP markers and found no significant defects in axon guidance (data not shown). *ptp-3(op147)* mutants displayed normal locomotion, feeding, defecation and egg-laying behavior.

With the caveat that *ptp-3(op147)* may not abolish PTP-3 function, these observations suggest that if *ptp-3* functions in axon guidance in *C. elegans* its functions are subtle or redundant.

### ***vab-1* and *ptp-3* mutations have synergistic effects on morphogenesis**

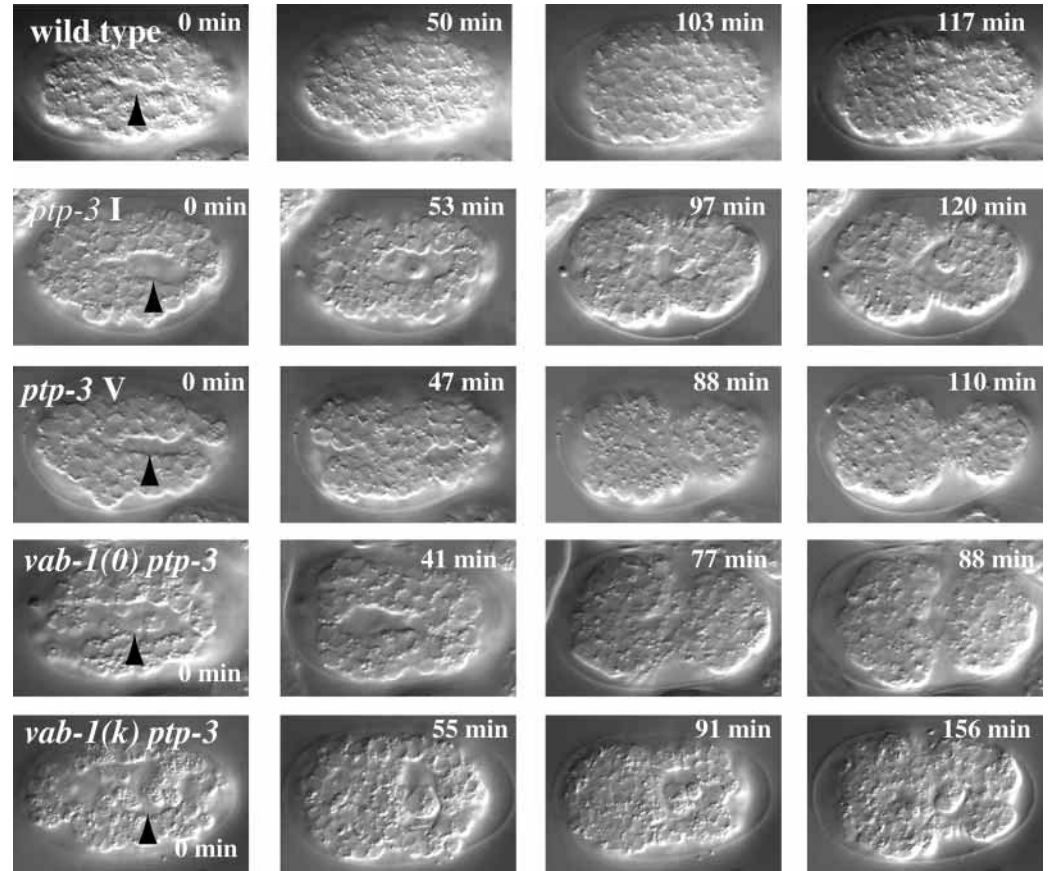
Our data show that PTP-3 signaling and VAB-1 Eph RTK signaling function in the same processes of embryonic morphogenesis. To ask whether *ptp-3* signaling interacted with Eph receptor signaling we constructed strains containing *ptp-3(op147)* and *vab-1* null [*vab-1(0)*] mutations. The *vab-1(0) ptp-3* double mutant strains displayed strongly enhanced morphogenetic defects compared to *vab-1* null mutants. *vab-1(0)* mutations alone result in approx. 50% embryonic lethality and approx. 80% total lethality (George et al., 1998); despite this high level of lethality, some animals are viable and fertile, and *vab-1* null mutant strains can be propagated as homozygotes. In contrast, *vab-1(0) ptp-3* double mutant animals were completely inviable and always arrested during embryogenesis. We analyzed the embryogenesis of such double mutants using 4-D microscopy, and found that all *vab-1(0) ptp-3* double mutant animals displayed severe defects in neuroblast movement during closure of the gastrulation cleft, and consistently arrested during early epidermal enclosure (Fig. 6, fourth row). These phenotypes correspond to the severe Class I phenotype, observed in a small fraction of *vab-1(0)* mutants (George et al., 1998). We did not observe any new morphogenetic phenotypes in the double mutants. Because the double mutants are more strongly affected than expected from additivity of mutant phenotypes these data indicate that VAB-1 and PTP-3 play related and partly redundant roles in morphogenesis.

The synergistic effects of *vab-1* and *ptp-3* mutations on morphogenesis could reflect their redundant function in the same set of cells or in different sets of cells. VAB-1 is expressed and required in neuroblasts and neurons during embryogenesis, whereas PTP-3 shows a more widespread distribution. We used tissue-specific promoters to ask whether PTP-3 function was required in neurons or in epidermal cells in a *vab-1 ptp-3* mutant background. Only expression of PTP-3 under the control of the pan-neural *unc-119* promoter caused a significant decrease in the lethality of *vab-1 ptp-3* double mutants (Fig. 5B). Expression of PTP-3 using epidermal promoters gave partial rescue that was not statistically significant. We conclude that one focus for the synergistic effects of VAB-1 and PTP-3 on epidermal development is the developing nervous system, although the partial rescue observed might indicate that PTP-3 functions in both neuronal and epidermal cells.

### **PTP-3 may function redundantly with kinase-dependent and kinase-independent functions of VAB-1**

Mutations predicted to eliminate VAB-1 kinase activity [*vab-1(k)* mutations] do not cause complete loss of VAB-1 function, leading to the model that VAB-1 has both kinase-dependent and kinase-independent functions (George et al., 1998). The kinase-independent function of VAB-1 may involve signaling via the ephrin VAB-2/EFN-1 (Chin-Sang et al., 1999; Wang et al., 1999). We used double mutant analysis to

**Fig. 6.** Time-lapse analysis of morphogenesis in *ptp-3* mutants and *vab-1 ptp-3* double mutants. Time series from five different embryos are shown: the first row is wild type; the second and third rows depict two representative *ptp-3*(*op147*) embryos; the fourth row shows a *vab-1(dx31) ptp-3*(*op147*) embryo (*vab-1(0)* double mutant), and the fifth row shows a typical *vab-1(e2) ptp-3*(*op147*) embryo (*vab-1(k)* double mutant). All panels are ventral views, with anterior to the left. First column: beginning of closure of the ventral gastrulation cleft (approx. 230–250 minutes after first cleavage); note the enlarged gastrulation cleft (arrowheads) in all mutant genotypes. Second column: later closure of gastrulation cleft. Third column: early epidermal enclosure. Fourth column: mid-epidermal enclosure. Times for each series are relative to the frame in the first column. Of the two *ptp-3* embryos shown, the upper series shows a severely affected embryo, with enlarged gastrulation cleft and early failure in epidermal enclosure; this animal arrested at the enclosure stage, corresponding to the Class I phenotype of *vab-1* mutants (George et al., 1998). The lower *ptp-3* series shows an embryo with slightly enlarged gastrulation cleft; this embryo underwent normal epidermal enclosure and hatched with normal morphology, corresponding to the Class V phenotype of *vab-1* or *vab-2* embryos. Both *vab-1 ptp-3* embryos shown displayed defects in gastrulation cleft closure and arrested at epidermal enclosure.



determine whether PTP-3 function is redundant with one or both of these VAB-1 pathways.

We found that the phenotypes of *vab-1* kinase mutants were dramatically enhanced by loss of *ptp-3* function (Fig. 6, Fig. 7A). *vab-1(k)* mutations in a *ptp-3*(+) background cause approx. 10% embryonic lethality (George et al., 1998), whereas *vab-1(k) ptp-3*(*op147*) double mutants displayed 80–100% embryonic lethality, depending on the *vab-1(k)* allele used. We analyzed *vab-1(k) ptp-3* double mutants using 4-D microscopy and confirmed that this enhancement was due to increased penetrance and severity of embryonic morphogenetic defects seen in the single mutants (Fig. 6, bottom row). We conclude that *ptp-3* functions redundantly with the kinase-dependent function of VAB-1.

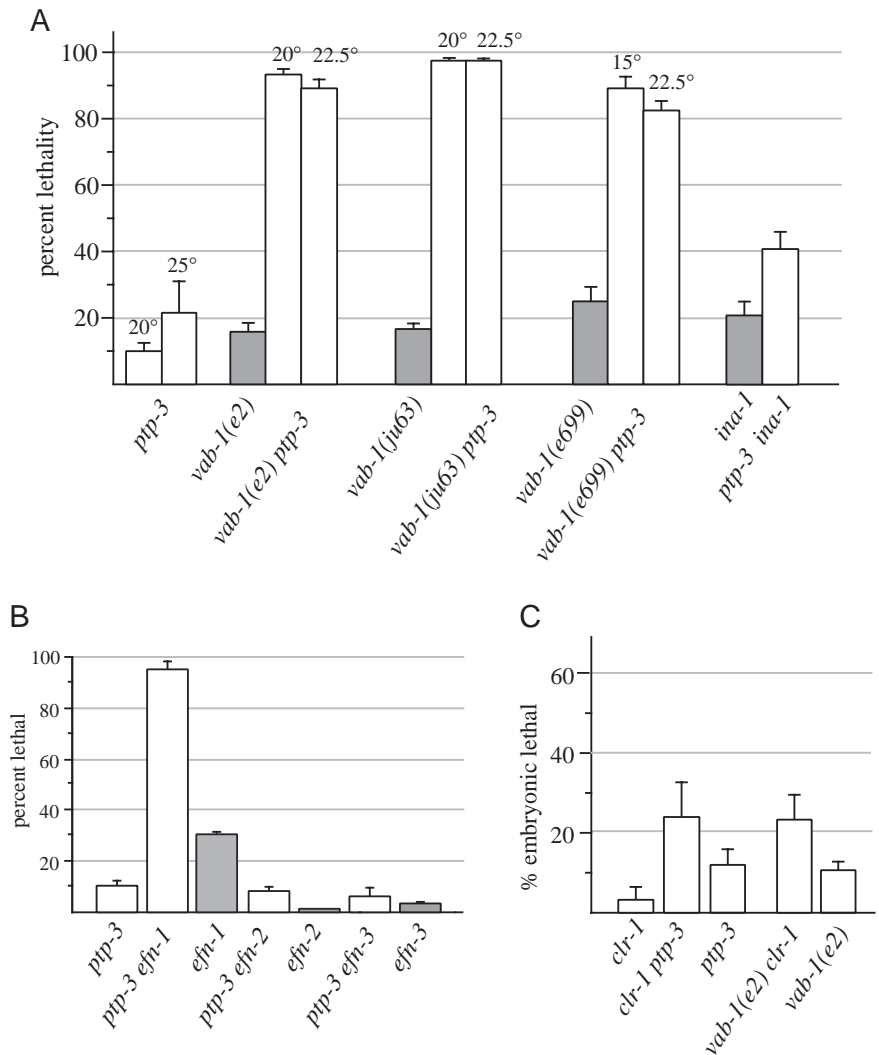
Because *vab-1(0) ptp-3* double mutants are more severely affected than *vab-1(k) ptp-3* double mutants, we reasoned that PTP-3 function must also be redundant with the VAB-1 kinase-independent pathway. To address this possibility we made double mutants between *ptp-3*(*op147*) and *vab-1* missense mutations affecting the extracellular domain. Extracellular domain missense alleles of VAB-1 such as *e699* cause stronger phenotypes than *vab-1(k)* alleles. However, *vab-1(e699)* showed weaker interactions with *ptp-3* than did the *vab-1(k)* alleles, although the double mutants were more severely affected than expected from additivity (Fig. 7A). These data

are consistent with PTP-3 also functioning redundantly with the kinase-independent function of VAB-1.

#### ***ptp-3* mutations synergize with *efn-1* ephrin mutations but not with *efn-2* or *efn-3* mutations**

From the synergistic genetic interactions of *ptp-3* and *vab-1* mutations we conclude that PTP-3 and VAB-1 play related and partly redundant roles in morphogenesis. We therefore investigated if PTP-3 displayed genetic interactions with the ephrin ligands for VAB-1. Mutations in three ephrins (EFN-1, EFN-2 and EFN-3) have been identified in *C. elegans*; genetic and biochemical analysis indicates that these ligands function in both the kinase-dependent and kinase-independent VAB-1 pathways (Chin-Sang et al., 1999; Wang et al., 1999). Mutations in the ephrin EFN-1 cause defects in gastrulation and epidermal enclosure similar to those of *vab-1* mutants. We found that *ptp-3; efn-1* double mutants displayed synergistic enhancement (Fig. 7B), although the double mutant strains displayed a different range of phenotypes from those of *vab-1(k) ptp-3* double mutants, in that many animals arrested during larval as opposed to embryonic development. EFN-1 may function both in VAB-1 kinase-dependent and kinase-independent pathways (Chin-Sang et al., 1999; Wang et al., 1999). The synergism of *ptp-3* with *vab-1(e699)* and with *efn-1* confirms that *ptp-3* function is redundant with both VAB-1 pathways.

**Fig. 7.** Synergism of *ptp-3* with *vab-1* and *vab-2* and lack of synergism with *ina-1* or *clr-1*. (A) Lethality was quantitated as described in Materials and Methods; error bars show s.e.m. Strains were raised at 20°C unless indicated. Data for *vab-1* are from George et al. (George et al., 1998). Strains doubly mutant for *ptp-3*(*op147*) and weaker *vab-1* kinase alleles (the missense alleles *e2* and *ju63*) showed partially penetrant synergistic lethality yet were viable as homozygotes; strains containing stronger kinase alleles were completely inviable as double mutants with *op147* (not shown). (B) Synergism of *ptp-3* with *efn* mutations. Data for *efn-1* from Chin-Sang et al. (Chin-Sang et al., 1999). Only *efn-1* displays synergistic lethality with *ptp-3*. Over 90% of the lethality in *vab-1*(kinase) *ptp-3* double mutants occurred during embryogenesis, whereas *vab-1*(*e699*) and *efn-1* double mutants displayed approx. 60% embryonic lethality and approx. 30% larval lethality. (C) Synergism of the RPTP *clr-1* with *vab-1* or *ptp-3* was tested using the temperature-sensitive *clr-1*(*e1745*), which is fully viable at 15°C and 20°C and is a fully penetrant late larval lethal at 25°C. *vab-1* *clr-1* homozygotes were viable at 20°C; *clr-1* *ptp-3* strains were viable at 15°C but not at 20°C, possibly suggestive of a mild enhancement of the Clr-1 phenotype. Embryonic lethality was quantitated using balanced strains of genotype *clr-1*/*mln1* *mls14*, *vab-1* *clr-1*/*mln1* *mls14*, and *clr-1* *ptp-3*/*mln1* *mls14*. Strains were raised at 25°C and the embryonic lethality of non-GFP-expressing animals quantitated.



The ephrins EFN-2 and EFN-3 have minor roles in embryogenesis, as loss of *efn-2* or *efn-3* function causes only mild defects in morphogenesis (Wang et al., 1999). *ptp-3*; *efn-2* and *ptp-3*; *efn-3* double mutants and a *ptp-3*; *efn-2*; *efn-3* triple mutant did not show synergistic enhancement of morphogenetic defects (Fig. 7B). We conclude that PTP-3 functions redundantly with EFN-1, but not with EFN-2 or EFN-3, in regulating embryonic morphogenesis.

### Specificity of the synergistic interaction of *vab-1* and *ptp-3* mutations

Does the synergistic enhancement of *vab-1* or *efn-1* phenotypes by *ptp-3* reflect a specific interaction between the VAB-1 Eph RTK and PTP-3/LAR pathways? To address this question, we first asked whether *ptp-3* displayed genetic interactions with another *C. elegans* RTK, the FGFR homolog EGL-15, which functions in cell migration (DeVore et al., 1995). We found that *ptp-3*; *egl-15* double mutants displayed additive phenotypes, in that *egl-15* egg-laying phenotypes were neither enhanced nor suppressed (data not shown), suggesting that PTP-3 does not function synergistically or antagonistically with EGL-15/FGFR signaling. Because LAR has been shown to negatively regulate insulin receptor signaling in cell culture (Kulas et al.,

1996), we also asked whether *ptp-3* displayed genetic interactions with the *C. elegans* insulin receptor homolog DAF-2 (Kimura et al., 1997). *daf-2* mutations cause a dauer-constitutive phenotype at 25°C; a *ptp-3*; *daf-2* double mutant strain also displayed a dauer-constitutive phenotype at the restrictive temperature (data not shown), suggesting that *ptp-3* may not repress insulin receptor signaling in *C. elegans*.

We also asked whether mutations in another RPTP displayed genetic interactions with *vab-1*. The only other *C. elegans* RPTP for which mutations are known is the Type II RPTP CLR-1, which functions antagonistically with EGL-15 (Kokel et al., 1998). *vab-1* *clr-1* double mutants displayed at most a mild enhancement of the *Vab-1* embryonic lethal phenotype; *clr-1* *ptp-3* double mutants similarly displayed a mild enhancement of *Ptp-3* phenotypes (Fig. 7C). In *Drosophila*, DLAR and the CLR-1-like phosphatase DPTP69D function redundantly in some contexts; in contrast, our data suggest that the incomplete penetrance of *ptp-3* or *vab-1* phenotypes does not reflect redundancy with CLR-1.

While these data suggest that the interaction of PTP-3 and VAB-1 reflects redundant functions of those specific pathways, it remained possible that loss of function in *ptp-3* might non-specifically enhance the defects of other epidermal

morphogenesis mutants. To address this possibility we made animals doubly mutant for *ptp-3* and a weak allele of the  $\alpha$ -integrin INA-1 (Baum and Garriga, 1997). Like VAB-1, INA-1 is expressed in the nervous system, and loss of *ina-1* function causes morphogenetic defects in the epidermis. We found that *ptp-3; ina-1* double mutants displayed additive effects (Fig. 7A). These data suggest that PTP-3 and INA-1 have independent functions in morphogenesis, and that loss of PTP-3 function does not enhance all morphogenetic mutants.

## DISCUSSION

### The evolution of LAR-like RPTPs

The LAR-like RPTPs have been highly conserved in animal evolution. LAR-like RPTPs have been identified in vertebrates, *Drosophila* (DLar), leeches (HmLAR1, HmLAR2), protochordates (Matthews et al., 1991), and now in nematodes. In all vertebrate species examined, three LAR subfamily RPTPs are expressed: LAR itself, and the closely related proteins PTP $\sigma$  and PTP $\delta$ . The *Drosophila* and *C. elegans* genomes each contain a single LAR-like gene, whereas the leech *Hirudo medicinalis* expresses two LAR-family genes, HmLAR1 and HmLAR2 (Gershon et al., 1998). Ancestral metazoans may thus have expressed a single LAR-like gene that became duplicated in the annelid and vertebrate lineages.

Vertebrate LAR subfamily genes are expressed in distinct but partly overlapping patterns, both in the developing and adult nervous systems and in a variety of non-neuronal tissues (Schaapveld et al., 1998). Like its vertebrate orthologs, PTP-3 displays widespread, almost ubiquitous expression in early *C. elegans* embryos. PTP-3 later becomes localized to neuronal processes, as found for other vertebrate and invertebrate LAR family members (e.g. Tian et al., 1991). Outside the nervous system LAR-like proteins are often found in proliferating epithelia, such as those of the lung and gut. In some mature *C. elegans* epidermal cells PTP3 appears to localize to adherens junctions; vertebrate LAR and PTP $\sigma$  proteins are also found in adherens junctions (Aicher et al., 1997), where they interact with  $\beta$ -catenin (Kypta et al., 1996). The potential role of PTP-3 in epidermal adherens junctions is unclear, as *ptp-3* mutant phenotypes do not resemble those resulting from loss of function in the catenin/cadherin complex (Costa et al., 1998); furthermore, loss of function in *ptp-3* did not enhance or suppress the phenotypes of loss-of-function mutations in other adherens junction proteins such as HMP-1 (data not shown).

Most LAR family genes generate multiple transcripts and encode multiple protein isoforms, although the way in which these isoforms arise is apparently not conserved between animal phyla. Vertebrate LAR, PTP $\sigma$ , and PTP $\delta$  genes all undergo alternative splicing involving exons encoding both extracellular and intracellular domains (O'Grady et al., 1994; Zhang and Longo, 1995). Many LAR family isoforms differ only within their extracellular domains, suggesting that the different isoforms could interact differently with ligands. For example, inclusion of a small exon within FNIII repeat 5 modulates the binding of LAR to laminin-nidogen (O'Grady et al., 1998).

We have shown that the *C. elegans ptp-3* gene encodes at least two isoforms, PTP-3A and PTP-3B, by use of alternative

promoters; this genomic organization has so far not been found in other LAR genes. Our anti-PTP-3 antibodies, which should recognize both isoforms, showed staining weaker than that of an isoform-specific PTP-3B::GFP transgene but otherwise indistinguishable, implying that both isoforms are expressed in similar patterns. The *ptp-3(op147)* insertion allele affects a phosphatase domain common to both isoforms and should decrease the function of both isoforms, although it may not affect phosphatase-independent functions of PTP-3, as proposed for *Drosophila* Lar (Maurel-Zaffran et al., 2001). Transgenes encoding only PTP-3B can rescue most or all of the defects observed in *ptp-3* mutants, suggesting that PTP-3B function is necessary for morphogenesis. Consistent with this hypothesis, a deletion mutation that specifically disrupts the PTP-3A isoform (K. Gengyo-Ando and S. Mitani, personal communication) does not cause defects in embryonic morphogenesis and does not synergize with *vab-1* mutations (data not shown). PTP-3A might have no function in embryonic morphogenesis, or its functions might be redundant with PTP-3B, such that only mutations disrupting both isoforms cause morphogenetic defects.

### The functions of LAR-like RPTPs

Work on *Drosophila* has established that LAR-like RPTPs function in axon guidance and fasciculation. In *Drosophila*, some Lar mutant phenotypes are synergistically enhanced in double mutant combinations with two other RPTPs, DPPT69D and DPPT99A, showing that the partial penetrance of LAR null mutant defects reflects redundant functions of these RPTPs (Desai et al., 1997). Genetic interactions indicate that in *Drosophila* neural RPTPs also function as positive regulators of Robo/Slit-based growth cone repulsion from the midline (Sun et al., 2000a). Mutations in murine LAR-like RPTPs cause subtle defects in neural tissues, although it is unclear if these reflect defects in axon guidance. The three vertebrate LAR-like RPTPs have overlapping expression patterns, suggesting that the subtle phenotypes of LAR, PTP $\sigma$ , and PTP $\delta$  mutants could reflect redundant functions of these RPTPs. We have found that in *C. elegans* LAR plays a subtle role in early neural and epidermal development, as reflected by the mild defects of *ptp-3* mutants. The mild phenotypes of LAR mutants in *Drosophila*, mice and *C. elegans* suggest the possibility that these proteins function in highly redundant signaling processes.

Our analysis of *ptp-3* mutant phenotypes has revealed that PTP-3 and Eph signaling are required in similar processes of embryogenesis. Loss of function in PTP-3, in the Eph receptor VAB-1, or in the ephrin ligand EFN-1, causes incompletely penetrant defects in neuroblast movements during closure of the gastrulation cleft, and in later epidermal morphogenesis. In *vab-1 ptp-3* double mutants the penetrance and severity of these defects are dramatically enhanced, although no new defects are seen in the double mutants. The simplest interpretation of this synergistic genetic interaction is that PTP-3 and VAB-1 function in closely related pathways, and that these pathways have partly redundant functions in controlling neuroblast movements. In contrast to the extremely variable defects of *vab-1(0)* or *ptp-3* single mutants, *vab-1(0) ptp-3* double mutants display a consistent arrest at early epidermal enclosure. This suggests that the variability of the single mutant phenotypes reflects compensation by the other

pathway; that is, the variability of the Vab-1 null phenotype reflects the ability of PTP-3 signaling to partly compensate for lack of VAB-1, and vice versa. The synergistic interaction of *ptp-3* with *efn-1* mutations is consistent with previous data showing that EFN-1 functions in the VAB-1 pathway in embryonic morphogenesis (Chin-Sang et al., 1999). *ptp-3* does not show similar synergistic lethal interactions with ephrins *efn-2* and *efn-3*, consistent with their relatively minor roles in embryogenesis (Wang et al., 1999).

Because *vab-1* and *ptp-3* mutants display defects in the movements of ventral neuroblasts during gastrulation cleft closure, we favor the hypothesis that VAB-1 and PTP-3 function redundantly within the same sets of neuronal precursors. This hypothesis is supported by our tissue-specific expression data. Significant rescue of *vab-1 ptp-3* mutant phenotypes was only observed when PTP-3B was expressed using a pan-neural promoter and not when using epithelial or epidermal-specific promoters. While these experiments do not address whether VAB-1 and PTP-3 function in the same individual neurons, they are consistent with VAB-1 and PTP-3 functioning in the same tissue. The incomplete rescue observed in these experiments could reflect failure to accurately reproduce the endogenous PTP-3 expression pattern, or it could reflect an additional role for PTP-3 in epidermal cells.

Several PTPs, including LMW-PTP, FAP-1, and SHP-2, appear to function downstream of Eph receptors (Lin et al., 1999; Miao et al., 2000; Stein et al., 1998). Although PTP-3 is unlikely to function directly in the VAB-1/Eph receptor signaling pathway, this is to our knowledge the first indication of a specific genetic interaction between a receptor-like PTP and Eph pathways. Our proposal that a receptor PTP and receptor PTK function redundantly in promoting signaling through a common pathway raises the question of the mechanism by which this may be achieved by two apparently antagonistic enzymes. While there are abundant examples of PTPs antagonizing PTK-dependent signaling pathways, there are also many examples of PTPs that function positively to promote signaling. For example, CD45, the prototypic receptor PTP, plays an essential positive role in signaling through T and B cell receptors (Neel, 1997) and PTP- $\alpha$  promotes signaling events associated with cell growth (Zheng et al., 1992). In both cases, the PTPs appear to dephosphorylate an inhibitory site of tyrosine phosphorylation at the C terminus of Src family PTKs, activating the kinase. Thus, a PTP can function in concert with a PTK to promote tyrosine phosphorylation. The SH2-domain-containing phosphatase SHP-2, and its *Drosophila* homologue Csw, function positively in several RTK pathways (Allard et al., 1996; Perkins et al., 1996). In the case of the RTK Torso, Csw can promote signaling by dephosphorylation of inhibitory phosphotyrosines in the Torso cytoplasmic domain (Cleghon et al., 1998). We think it unlikely that PTP-3 acts via dephosphorylation of VAB-1, as PTP-3 mutations have dramatic effects in a VAB-1 null mutant background. PTP-3 might promote signaling in the VAB-1 pathway by dephosphorylation of a downstream substrate; elucidation of the substrates of PTP-3 will be required to test this possibility.

LAR-like RPTPs and Eph RTKs have been implicated in related aspects of cellular behavior in other organisms. Both Eph RTKs and LAR can cause axonal growth cone collapse (Baker and Macagno, 2000; Drescher et al., 1995), and thus can promote repulsive interactions between growth cones and

their substrates (Orioli and Klein, 1997). However, in some situations LAR-like RPTPs may promote cell adhesion or growth-cone attraction, rather than repulsion (e.g. Sun et al., 2000b), suggesting that Eph signaling and LAR signaling could play antagonistic or synergistic roles depending on the specific cellular context. Our finding that Eph signaling and LAR play related and partly redundant roles in *C. elegans* morphogenesis suggests that these two pathways may also be intimately connected in other organisms.

We thank Inessa Grinberg and Julie McCleery for making and characterizing some *ptp-3* double mutants, and Stephanie Kyriakopoulos for help integrating *ptp-3* transgenes. Some strains used in this work were provided by the *Caenorhabditis* Genetics Center, which is funded by the NIH National Center for Research Resources (NCRR). The balancer chromosome *mIn1* was developed by the *C. elegans* Genetic Toolkit project, which is funded by a grant from the NIH NCRR to Ann M. Rose, David L. Baillie, and Donald L. Riddle. We thank Andy Fire for sharing GFP vectors. We are very grateful to Al Zahler for gifts of worm mRNA and advice on RT-PCR, Doug Kellogg and the Kellogg lab for protein purification protocols, and Bill Sullivan for help with confocal microscopy. We thank members of the Chisholm and Jin labs for help and discussions, especially Ian Chin-Sang for help with antibody staining. We thank Renee Baran, Ian Chin-Sang, Grant Hartzog, Yishi Jin, and Al Zahler for comments on this manuscript. This work was funded by NIH grants GM55989 (N.T.) and GM54657 (A.D.C.) and from the UC Biotechnology Training Program; A.D.C. is an Alfred P. Sloan Fellow in the Neurosciences.

## REFERENCES

- Aicher, B., Lerch, M. M., Muller, T., Schilling, J. and Ullrich, A. (1997). Cellular redistribution of protein tyrosine phosphatases LAR and PTPsigma by inducible proteolytic processing. *J. Cell. Biol.* **138**, 681-696.
- Allard, J. D., Chang, H. C., Herbst, R., McNeill, H. and Simon, M. A. (1996). The SH2-containing tyrosine phosphatase corkscrew is required during signaling by sevenless, Ras1 and Raf. *Development* **122**, 1137-1146.
- Baker, M. W. and Macagno, E. R. (2000). The role of a LAR-like receptor tyrosine phosphatase in growth cone collapse and mutual-avoidance by sibling processes. *J. Neurobiol.* **44**, 194-203.
- Bateman, J., Reddy, R. S., Saito, H. and Van Vactor, D. (2001). The receptor tyrosine phosphatase Dlar and integrins organize actin filaments in the *Drosophila* follicular epithelium. *Curr. Biol.* **11**, 1317-27.
- Bateman, J., Shu, H. and Van Vactor, D. (2000). The guanine nucleotide exchange factor trio mediates axonal development in the *Drosophila* embryo. *Neuron* **26**, 93-106.
- Baum, P. D. and Garriga, G. (1997). Neuronal migrations and axon fasciculation are disrupted in *ina-1* integrin mutants. *Neuron* **19**, 51-62.
- Brady-Kalnay, S. M. and Tonks, N. K. (1995). Protein tyrosine phosphatases as adhesion receptors. *Curr. Opin. Cell. Biol.* **7**, 650-657.
- Carroll, C. W., Altman, R., Schieltz, D., Yates, J. R. and Kellogg, D. (1998). The septins are required for the mitosis-specific activation of the Gin4 kinase. *J. Cell. Biol.* **143**, 709-717.
- Chin-Sang, I. D., George, S. E., Ding, M., Moseley, S. L., Lynch, A. S. and Chisholm, A. D. (1999). The ephrin VAB-2/EFN-1 functions in neuronal signaling to regulate epidermal morphogenesis in *C. elegans*. *Cell* **99**, 781-790.
- Clandinin, T. R., Lee, C. H., Herman, T., Lee, R. C., Yang, A. Y., Ovasapyan, S. and Zipursky, S. L. (2001). *Drosophila* LAR Regulates R1-R6 and R7 Target Specificity in the Visual System. *Neuron* **25**, 237-248.
- Cleghon, V., Feldmann, P., Ghiglione, C., Copeland, T. D., Perrimon, N., Hughes, D. A. and Morrison, D. K. (1998). Opposing actions of CSW and RasGAP modulate the strength of Torso RTK signaling in the *Drosophila* terminal pathway. *Mol. Cell* **2**, 719-727.
- Costa, M., Raich, W., Agbunag, C., Leung, B., Hardin, J. and Priess, J. R. (1998). A putative catenin-cadherin system mediates morphogenesis of the *Caenorhabditis elegans* embryo. *J. Cell. Biol.* **141**, 297-308.

- den Hertog, J., Blanchetot, C., Buist, A., Overvoorde, J., van der Sar, A. and Tertoolen, L. G. (1999). Receptor protein-tyrosine phosphatase signalling in development. *Int. J. Dev. Biol.* **43**, 723-733.
- Desai, C. J., Gindhart, J. G., Jr., Goldstein, L. S. and Zinn, K. (1996). Receptor tyrosine phosphatases are required for motor axon guidance in the *Drosophila* embryo. *Cell* **84**, 599-609.
- Desai, C. J., Krueger, N. X., Saito, H. and Zinn, K. (1997). Competition and cooperation among receptor tyrosine phosphatases control motoneuron growth cone guidance in *Drosophila*. *Development* **124**, 1941-1952.
- DeVore, D. L., Horvitz, H. R. and Stern, M. J. (1995). An FGF receptor signaling pathway is required for the normal cell migrations of the sex myoblasts in *C. elegans* hermaphrodites. *Cell* **83**, 611-620.
- Drescher, U., Kremoser, C., Handwerker, C., Loschinger, J., Noda, M. and Bonhoeffer, F. (1995). In vitro guidance of retinal ganglion cell axons by RAGS, a 25 kDa tectal protein related to ligands for Eph receptor tyrosine kinases. *Cell* **82**, 359-370.
- Edgley, M. L. and Riddle, D. L. (2001). LG II balancer chromosomes in *Caenorhabditis elegans*: *mT1(II;III)* and the *mIn1* set of dominantly and recessively marked inversions. *Mol. Genet. Genomics* **266**, 385-395.
- Eide, D. and Anderson, P. (1988). Insertion and excision of *Caenorhabditis elegans* transposable element *Tc1*. *Mol. Cell. Biol.* **8**, 737-746.
- Elchebly, M., Wagner, J., Kennedy, T. E., Lancot, C., Michalyszyn, E., Itie, A., Drouin, J. and Tremblay, M. L. (1999). Neuroendocrine dysplasia in mice lacking protein tyrosine phosphatase  $\sigma$ . *Nat. Genet.* **21**, 330-333.
- Finney, M. and Ruvkun, G. (1990). The *unc-86* gene product couples cell lineage and cell identity in *C. elegans*. *Cell* **63**, 895-905.
- Fitzpatrick, K. A., Gorski, S. M., Ursuliak, Z. and Price, J. V. (1995). Expression of protein tyrosine phosphatase genes during oogenesis in *Drosophila melanogaster*. *Mech. Dev.* **53**, 171-183.
- Frydman, H. M. and Spradling, A. C. (2001). The receptor-like tyrosine phosphatase *lar* is required for epithelial planar polarity and for axis determination within ovarian follicles. *Development* **128**, 3209-3220.
- Garrity, P. A., Lee, C. H., Salecker, I., Robertson, H. C., Desai, C. J., Zinn, K. and Zipursky, S. L. (1999). Retinal axon target selection in *Drosophila* is regulated by a receptor protein tyrosine phosphatase. *Neuron* **22**, 707-717.
- George, S. E., Simokat, K., Hardin, J. and Chisholm, A. D. (1998). The VAB-1 Eph receptor tyrosine kinase functions in neural and epithelial morphogenesis in *C. elegans*. *Cell* **92**, 633-643.
- Gershon, T. R., Baker, M. W., Nitabach, M., Wu, P. and Macagno, E. R. (1998). Two receptor tyrosine phosphatases of the LAR family are expressed in the developing leech by specific central neurons as well as select peripheral neurons, muscles, and other cells. *J. Neurosci.* **18**, 2991-3002.
- Gutch, M. J., Flint, A. J., Keller, J., Tonks, N. K. and Hengartner, M. O. (1998). The *Caenorhabditis elegans* SH2 domain-containing protein tyrosine phosphatase PTP-2 participates in signal transduction during oogenesis and vulval development. *Genes Dev.* **12**, 571-585.
- Harlow, E. and Lane, D. (1999). *Using Antibodies: A Laboratory Manual*. Cold Spring Harbor, NY: Cold Spring Harbor Laboratory Press.
- Kimura, K. D., Tissenbaum, H. A., Liu, Y. and Ruvkun, G. (1997). *daf-2*, an insulin receptor-like gene that regulates longevity and diapause in *Caenorhabditis elegans*. *Science* **277**, 942-946.
- Kokel, M., Borland, C. Z., DeLong, L., Horvitz, H. R. and Stern, M. J. (1998). *clr-1* encodes a receptor tyrosine phosphatase that negatively regulates an FGF receptor signaling pathway in *Caenorhabditis elegans*. *Genes Dev.* **12**, 1425-1437.
- Krueger, N. X., Van Vactor, D., Wan, H. I., Gelbart, W. M., Goodman, C. S. and Saito, H. (1996). The transmembrane tyrosine phosphatase DLAR controls motor axon guidance in *Drosophila*. *Cell* **84**, 611-622.
- Kulas, D. T., Goldstein, B. J. and Mooney, R. A. (1996). The transmembrane protein-tyrosine phosphatase LAR modulates signaling by multiple receptor tyrosine kinases. *J. Biol. Chem.* **271**, 748-754.
- Kypta, R. M., Su, H. and Reichardt, L. F. (1996). Association between a transmembrane protein tyrosine phosphatase and the cadherin-catenin complex. *J. Cell. Biol.* **134**, 1519-1529.
- Lin, D., Gish, G. D., Songyang, Z. and Pawson, T. (1999). The carboxyl terminus of B class ephrins constitutes a PDZ domain binding motif. *J. Biol. Chem.* **274**, 3726-3733.
- Matthews, R. J., Flores, E. and Thomas, M. L. (1991). Protein tyrosine phosphatase domains from the protochordate *Styela plicata*. *Immunogenetics* **33**, 33-41.
- Maurel-Zaffran, C., Suzuki, T., Gahnon, G., Treisman, J., E. and Dickson, B., Jr. (2001). Cell-autonomous and -nonautonomous functions of LAR in R7 photoreceptor axon targeting. *Neuron* **32**, 225-235.
- Miao, H., Burnett, E., Kinch, M., Simon, E. and Wang, B. (2000). Activation of EphA2 kinase suppresses integrin function and causes focal adhesion-kinase dephosphorylation. *Nat. Cell. Biol.* **2**, 62-69.
- Neel, B. G. (1997). Role of phosphatases in lymphocyte activation. *Curr. Opin. Immunol.* **9**, 405-420.
- O'Grady, P., Krueger, N. X., Streuli, M. and Saito, H. (1994). Genomic organization of the human LAR protein tyrosine phosphatase gene and alternative splicing in the extracellular fibronectin type-III domains. *J. Biol. Chem.* **269**, 25193-25199.
- O'Grady, P., Thai, T. C. and Saito, H. (1998). The laminin-nidogen complex is a ligand for a specific splice isoform of the transmembrane protein tyrosine phosphatase LAR. *J. Cell. Biol.* **141**, 1675-1684.
- Orioli, D. and Klein, R. (1997). The Eph receptor family: axonal guidance by contact repulsion. *Trends Genet.* **13**, 354-359.
- Perkins, L. A., Johnson, M. R., Melnick, M. B. and Perrimon, N. (1996). The nonreceptor protein tyrosine phosphatase corkscrew functions in multiple receptor tyrosine kinase pathways in *Drosophila*. *Dev. Biol.* **180**, 63-81.
- Plowman, G. D., Sudarsanam, S., Bingham, J., Whyte, D. and Hunter, T. (1999). The protein kinases of *Caenorhabditis elegans*: a model for signal transduction in multicellular organisms. *Proc. Natl. Acad. Sci. USA* **96**, 13603-13610.
- Pulido, R., Serra-Pagès, C., Tang, M. and Streuli, M. (1995). The LAR/PTP $\delta$ /PTP $\sigma$  subfamily of transmembrane protein-tyrosine-phosphatases: multiple human LAR, PTP $\delta$ , and PTP $\sigma$  isoforms are expressed in a tissue-specific manner and associate with the LAR-interacting protein LIP1. *Proc. Natl. Acad. Sci. USA* **92**, 11686-11690.
- Ren, J. M., Li, P. M., Zhang, W. R., Sweet, L. J., Cline, G., Shulman, G. I., Livingston, J. N. and Goldstein, B. J. (1998). Transgenic mice deficient in the LAR protein-tyrosine phosphatase exhibit profound defects in glucose homeostasis. *Diabetes* **47**, 493-497.
- Riddle, D., Blumenthal, T., Meyer, B. J. and Priess, J. R. (1997). *C. elegans* II. Cold Spring Harbor, NY: Cold Spring Harbor Laboratory Press.
- Rushforth, A. M. and Anderson, P. (1996). Splicing removes the *Caenorhabditis elegans* transposon *Tc1* from most mutant pre-mRNAs. *Mol. Cell. Biol.* **16**, 422-429.
- Sambrook, J., Fritsch, E. F. and Maniatis, T. (1989). *Molecular Cloning: A Laboratory Manual*. New York: Cold Spring Harbor Laboratory Press.
- Schaapveld, R. Q., Schepens, J. T., Bachner, D., Attema, J., Wieringa, B., Jap, P. H. and Hendriks, W. J. (1998). Developmental expression of the cell adhesion molecule-like protein tyrosine phosphatases LAR, RPTP $\delta$  and RPTP $\sigma$  in the mouse. *Mech. Dev.* **77**, 59-62.
- Schaapveld, R. Q., Schepens, J. T., Robinson, G. W., Attema, J., Oerlemans, F. T., Franssen, J. A., Streuli, M., Wieringa, B., Hennighausen, L. and Hendriks, W. J. (1997). Impaired mammary gland development and function in mice lacking LAR receptor-like tyrosine phosphatase activity. *Dev. Biol.* **188**, 134-146.
- Serra-Pagès, C., Kedersha, N. L., Fazikas, L., Medley, Q., Debant, A. and Streuli, M. (1995). The LAR transmembrane protein tyrosine phosphatase and a coiled-coil LAR-interacting protein co-localize at focal adhesions. *EMBO J.* **14**, 2827-2838.
- Stein, E., Lane, A. A., Cerretti, D. P., Schoeckmann, H. O., Schroff, A. D., Van Etten, R. L. and Daniel, T. O. (1998). Eph receptors discriminate specific ligand oligomers to determine alternative signaling complexes, attachment, and assembly responses. *Genes Dev.* **12**, 667-678.
- Stoker, A. and Dutta, R. (1998). Protein tyrosine phosphatases and neural development. *BioEssays* **20**, 463-472.
- Sun, Q., Bahri, S., Schmid, A., Chia, W. and Zinn, K. (2000a). Receptor tyrosine phosphatases regulate axon guidance across the midline of the *Drosophila* embryo. *Development* **127**, 801-812.
- Sun, Q. L., Wang, J., Bookman, R. J. and Bixby, J. L. (2000b). Growth cone steering by receptor tyrosine phosphatase delta defines a distinct class of guidance Cue. *Mol. Cell. Neurosci.* **16**, 686-695.
- Tian, S. S., Tsoulfas, P. and Zinn, K. (1991). Three receptor-linked protein-tyrosine phosphatases are selectively expressed on central nervous system axons in the *Drosophila* embryo. *Cell* **67**, 675-680.
- Timmons, L. and Fire, A. (1998). Specific interference by ingested dsRNA. *Nature* **395**, 854.
- Uetani, N., Kato, K., Ogura, H., Mizuno, K., Kawano, K., Mikoshiba, K., Yakura, H., Asano, M. and Iwakura, Y. (2000). Impaired learning with enhanced hippocampal long-term potentiation in PTPdelta-deficient mice. *EMBO J.* **19**, 2775-2785.
- Wälchli, S., Colinge, J. and Hoof van Huijsdijnen, R. (2000). MetaBlasts:

- tracing protein tyrosine phosphatase gene family roots from Man to *Drosophila melanogaster* and *Caenorhabditis elegans* genomes. *Gene* **253**, 137-143.
- Wallace, M. J., Batt, J., Fladd, C. A., Henderson, J. T., Skarnes, W. and Rotin, D.** (1999). Neuronal defects and posterior pituitary hypoplasia in mice lacking the receptor tyrosine phosphatase PTP $\sigma$ . *Nat. Genet.* **21**, 334-338.
- Wang, X., Roy, P. J., Holland, S. J., Zhang, L. W., Culotti, J. G. and Pawson, T.** (1999). Multiple ephrins control cell organization in *C. elegans* using kinase-dependent and -independent functions of the VAB-1 Eph receptor. *Mol. Cell* **4**, 903-913.
- Wills, Z., Bateman, J., Korey, C. A., Comer, A. and Van Vactor, D.** (1999). The tyrosine kinase Abl and its substrate enabled collaborate with the receptor phosphatase Dlar to control motor axon guidance. *Neuron* **22**, 301-312.
- Yeo, T. T., Yang, T., Massa, S. M., Zhang, J. S., Honkaniemi, J., Butcher, L. L. and Longo, F. M.** (1997). Deficient LAR expression decreases basal forebrain cholinergic neuronal size and hippocampal cholinergic innervation. *J. Neurosci. Res.* **47**, 348-360.
- Zhang, J. S., Honkaniemi, J., Yang, T., Yeo, T. T. and Longo, F. M.** (1998). LAR tyrosine phosphatase receptor: a developmental isoform is present in neurites and growth cones and its expression is regional- and cell-specific. *Mol. Cell. Neurosci.* **10**, 271-286.
- Zhang, J. S. and Longo, F. M.** (1995). LAR tyrosine phosphatase receptor: alternative splicing is preferential to the nervous system, coordinated with cell growth and generates novel isoforms containing extensive CAG repeats. *J. Cell. Biol.* **128**, 415-431.
- Zheng, X. M., Wang, Y. and Pallen, C. J.** (1992). Cell transformation and activation of pp60c-src by overexpression of a protein tyrosine phosphatase. *Nature* **359**, 336-339.